P-42

PLASTIC WASTE AS A GOOD RAW MATERIAL FOR DESIGN MODULAR FLOOD BARRIER

ĽUBOMÍR ŠOOŠ, JURAJ ONDRUŠKA, PETER BIATH, VILIAM ČAČKO, MILOŠ MATÚŠ, MICHAL ČEKAN, PETER KRIZAN, and JURAJ BENIAK

Faculty of mechanical engineering STU in Bratislava, Nám. Slobody 17, 812 31 Bratislava, Slovakia
lubomir.soos@stuba.sk

The Slovak university of technology in Bratislava is currently involved in the project "Research of progressive technologies for the recovery of waste from scrap automobiles"[1] , in harmony with the priorities of the Slovak ministry of environment (SME). The principal coordinator of the project is the faculty of mechanical engineering, and the project is financed by the Recycling fund in Slovakia. SME has stated in a press release that: "foremost, the effective protection against flooding, and the reduction of environmental burdens in sensitive and national park zones remain our priority". (SME, Ing. Peter Žiga, PhD., press release ME SR, 1.7.2012.)."

Design of flood barrier

The basic requirements for the new barrier were that it would be: produced from recycled materials, self-anchoring but not permanently anchored to the ground, could be used on firm and soft ground, allow for convex and concave configurations, can copy rough terrain, can be easily deployed and removed, and can adjust the barriers height. The investigators filed a utility model application no. SK 5847 Y12 entitled "Modular flood barrier structure"[2].

If the barriers are installed on firm ground, then a rubber seal, designed from waste rubber, is placed below the horizontal parts of both water barriers. Connecting the vertical parts is done by using attachment bars. To obtain greater stability, the vertical parts are mounted to each other in a pattern. In the case that the barriers are located on uneven or soft ground, then anchoring pikes are used on the horizontal parts.

Before the development of the prototype, it was necessary to define the conditions under which the development team could determine appropriate solutions. In terms of innovative structural design, it was necessary to take into consideration some important factors: cost of production, assembly and disassembly, internal and external stability, flexibility, storage, and risk and safety. These factors have been attributed in the development process according to the importance of each one. Based on the comprehensive assessment of the whole structure the final design of the structure was proposed.

For a better understanding of the system, some important structural characteristics are considered. In order to maximize the strength of the barrier wall with a sloping height of 2 m, a pattern arrangement of two different block sizes is proposed (0,5 and 1 m blocks). The plastic half blocks are made by dividing larger 1×1 m blocks. In order to connect the blocks together in the vertical direction, a figure-eight connection concept is adopted (Fig. 2). In this way, a connection is created which ensures adequate strength, flexibility, and ease of connection in even the toughest of conditions. It also allows for a large difference (vertical movement – adaptability to varying terrain) between each individual block. In order to reduce excessive leaks between the blocks, terrain, and walls, a UV resistant sleeve made of sufficiently strong sheets was designed. These sheets are a cost effective solution

Anchoring the support rods (Fig. 5) to the plastic blocks is designed to be relatively simple, but also sufficient in distributing load onto the double rib section of the blocks. The

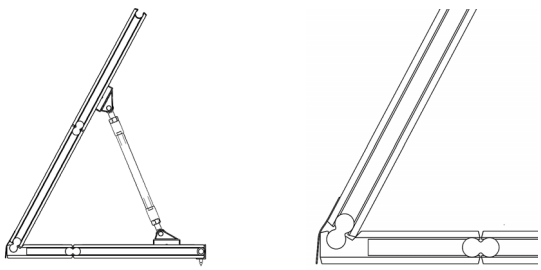

Fig. 1. **First virtual concept made from plastic**

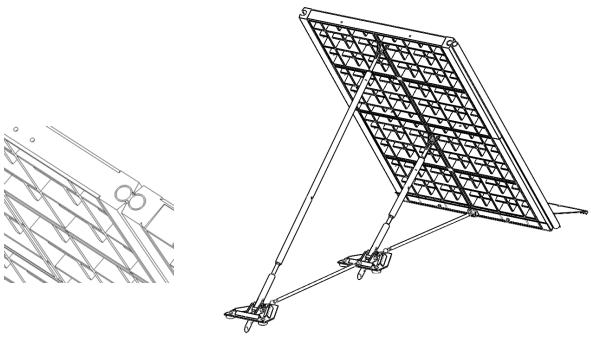

Fig. 2. **Modular structure of flood barrier, "figure-eight" connection**

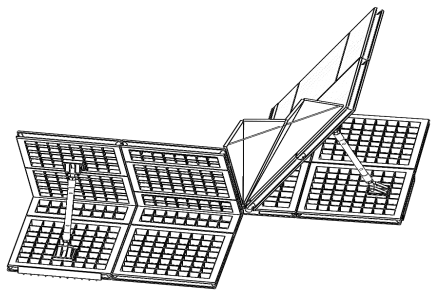

Fig. 3. **First virtual concept made from plastic**

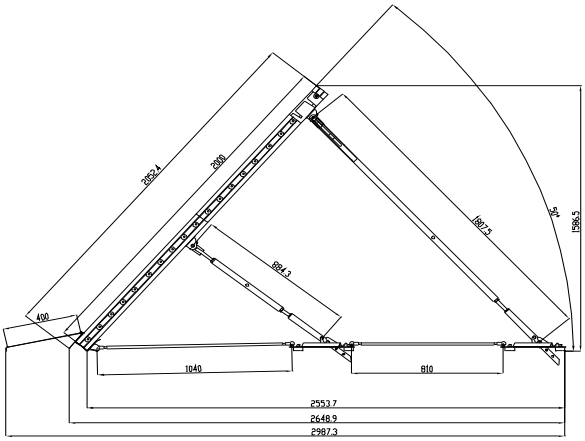

Fig. 4. **Dimensions of the modular flood barrier "side-view"**

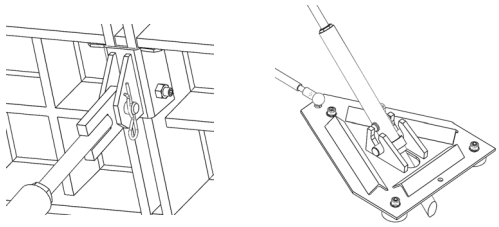

Fig. 5. **Structural nodes for support anchorage**

Fig. 6. **Static test under real conditions of hydrostatic loading in canal**

Fig. 7. **"Pool" test for the verification of maximum hydrostatic load**

length of the bracings can be adjusted in operation or in flooded conditions. Based on the calculations of internal and external stability, a flap is incorporated at the point of highest hydrostatic pressure which greatly increases safety. The FEA analysis of the structure and its individual parts allowed for calculating the optimal compromise between weight, strength, and geometry. The pattern structure of the plastic blocks connected by figure eight bars was structurally assessed. Based on the results, a simplification was designed for the length of the figure eight bars which were reduced to 700 mm which significantly simplifies the assembly and disassembly of the system.

An extendable tip provides versatility in anchoring in different types of terrain (Fig. 5).

After processing the necessary drawings and verifying the analysis results, a test sample for field testing of the flood protection system was produced.

Flood test by hydrostatic pressure

In the first stage of the projects realization, the investigators were able to develop a modular structure for flood barriers made from difficult to recover recycled materials. This is important, mainly in the recovery of composite materials from scrap automobiles. Parts of the prototype structure have been made at Chemosvit Environchem, a.s. and at the centre of innovation at STU. The investigators, in the first stage, decided to test the flood barriers with hydrostatic pressure to verify the theoretical basis of the design.

The flood test itself underwent a comprehensive analysis for determining where these tests would be performed. It was necessary to have a test site which encompassed the shape of the canal, its surface, water source, and above all, its safety and elimination of possible damage if the structure suddenly failed. As a result of the search for a suitable location to test the systems ability to withstand real conditions of water pressure and verify the stability of the individual modules, two tests were carried out at the water dam in Vištuk by Pezinok, Slovakia.

The first test was to erect a 3.6 m wide barrier on a rocky base with relatively perpendicular walls (Fig. 6). This test required that barrier to be assembled in one of the overflow canals by the dam. The second test involved constructing a square pool with the dimensions 3 × 3 meters entirely with the developed water barrier units (Fig. 7). Water was then pumped into the pool from a nearby source and filled to the intended max height of 160 cm. This test verified the integrity of the designed flood barrier at maximum water level for all criteria mentioned above. The ground consisted of a wet grass field which verified the ability of the barrier to be deployed in uneven terrain. The third, dry test was realized at a conference "Technology for environmental protection" – TOP2012.

Conclusion

Both verification tests obtained very positive results which complimented the designed structure and indicated that the flood barrier which was developed behaved very well under its intended operation.

This contribution/publication is the result of the project implementation: National Center for Research and Application of Renewable Energy Sources, ITMS 26240120016 supported by the Research & Development Operational Programme funded by the ERDF.

REFERENCES

1. Šooš Ľubomír, a kol.: Research of progressive waste recovery technologies for scrap vehicles, Project Recycling fund, April 2011.
2. Šooš Ľ., Prikkel K., Ondruška J., Olekšák J.: Modular structure of flood barrier. 16 s. : No. *Utility model: 5847 SK*, Effective as of: 19.8. 2011 (2011).

P-43

PRACTICAL USE OF LASER TECHNOLOGIES IN FIELD OF PLASTICS

LIBUŠE SÝKOROVÁ*, OLDŘICH ŠUBA, and JANA KNEDLOVÁ

Tomas Bata University in Zlin, Faculty of Technology, Department of Production Engineering, T. G. Masaryka 275, 762 72 Zlín, Czech Republic
sykorova@ft.utb.cz

Abstract

The paper deals with optimal adjust parameters of laser beam for laser marking of polymers. Commercial CO2 laser Mercury L-30 by firm LaserPro, USA was used for experimental describing. It was selected 5 basic of sorts covering materials, which was performed laser marking of text. The specimens were inspected and their characteristics were investigated. At last economic comparison of laser technologies and gold stamping no manual press was performed.

Introduction

Engraving belongs among non-conventional method of laser scribing that are based mainly on the physical or the physic-chemical principle of stock removal without the action of force on the machined material. This study deals with optimal setting of parameters of laser beam for booking scribing.

Experiment

Commercial CO2 laser Mercury L-30 by firm LaserPro, USA was used for experiment. It is possible to change power and feed rate of laser system. Ray of laser could be focused on mark diameter d = 185 μm. The maximum value of power is 30 W and maximum value of feed is 1066 mm s^{-1}. Laser is machining with the software help of Corel Draw. Wide spectrum of different materials (ceramic, quartz, plastic, rubber, wood and certain composite structures) can be scribed and machined by laser MERCURY L-30. This laser type is used mainly for commercial engraving.

Table I
Covering materials used for experiments

N.	Material title	Colour	Surface	Description
1	BALADEK	dark-blue	roughened of slight grooves	leather imitation
2	BALADEK	vinous	smooth without visible defects	leather imitation
3	IMPERIAL	green	visible cross and lengthwise fibrous structure	natural buckram
4	IMPERIAL	red	visible cross and lengthwise fibrous structure	natural buckram
5	COVERING PAPER	blue	rough, visible relief	properties like hard paper
6	NATURAL	white-grey	markedly visible structure fibrous	tow-cloth

5 basic types of covering materials were selected for experiment. These samples were scribed by laser. Each material differed from others by its colour, surface and structure – see Table I.

Experimental text was scribed with parameters combination of laser system – maximum feed 100% (1066 mm/s) and power was being changed – see Table II (ref.[1,4]).

Due to space limit is in paper showed only one described material IMPERIAL green – see Fig. 1.

Optimal parameters combination of laser system

Value of input characteristics are stated as a percents from maximal power (pmax=30W) and maximal feed (fmax=1066mm/s) – see table III.

Table II
Selected technological parameters for the experiment

Feed f [%]	Feed f [mm/s]	Power [%]	Power P [W]
100	1066	10	3
100	1066	7	2,1
100	1066	20	6
100	1066	40	12
100	1066	60	18
100	1066	80	24

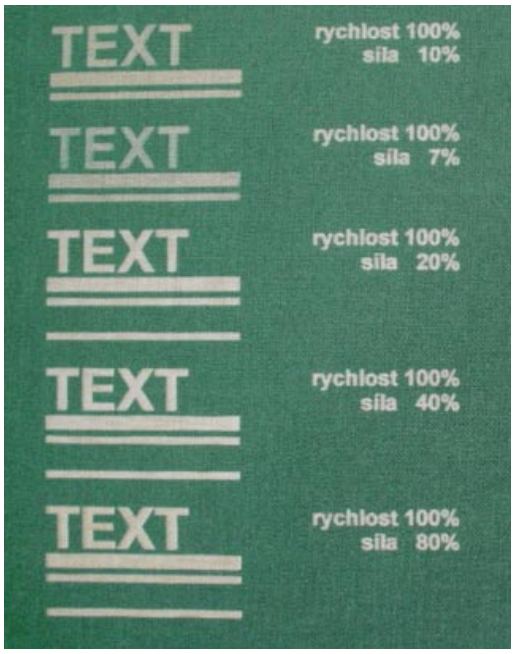

Fig. 1. **IMPERIAL (green)**

Table III
Optimal parameters combination of laser system for used materials

N.	Material title	Optimal feed	Optimal power	Annotation
1	BALADEK	100%	40-50%	Narrow interval of power is caused especially by properties of material surface layer
2	BALADEK	100%	40-80%	Power range mainly depends on required text colour
3	IMPERIAL	100%	20-80%	Text is even legible with power value under 20%
4	IMPERIAL	100%	20-80%	Text parameters are same as for the previous material
5	COVERING PAPER	100%	5-20%	Suitable for lower power value. The material began burn at power over 40%
6	NATURAL	100%	40-50%	Suitable for higher power - over 40%

Economic evaluation of laser scribing usage

The laser technology is usually used everywhere cannot be using conventional method of machining. The fast changes of working cycle can be applied with advantage by the laser system. It is possible to achieve high level of productivity with rapid symbol change in program Corel Draw[1,4].

Advantages of usage of laser system:
- good working conditions for machine operator
- silent running
- higher safety of work than conventional machining
- reduction man power and production place
- stock removal without the action of force on the machined material
- nearly maintenance-free

Disadvantages of usage of laser system:
- too high actual price of laser system
- necessity of the evaporated material exhaust
- difficult reparation in case of laser machine damage
- colour of the text is affected only by the character of some layers of used material

Economic comparison of laser technologies and manual gold stamping of a thesis title part

From experimental results it is possible to state the laser scribing of title part of thesis took about 4 minutes – attributable costs are about 0,5 EU.

It was also observed that the scribing time with common technology of manual gold stamping would take about 60 minutes – attributable costs are about 5 EU (ref.[1,4]).

Conclusion

From table is evident it is not necessary used lower feed than maximal for bookbinding laser scribing. Laser is capable to create desired text on the material surface even by low power value. Hence, it is not necessary to lower laser feed from the point of view productivity.

It is necessary to know suitable output parameters setting of specific laser system and properties of machined materials for obtaining good results of scribing by laser.

Furthermore, it was observed the laser power and properties of particular material layers have biggest influence on properties and appearance of scribing text. The optimal setting laser power in interval 40–50 % from maximal power of the laser machine was possible to use for almost all covering materials. Only covering paper was different because its properties are rather similar to normal paper than textile or imitation of leather.

Influence of the covering material colour was last factor which was evaluated. It was observed the colour does not influence properties and appearance of scribing text.

It stands to reason that technologies utilizing of laser beam are severalfold faster than gold stamping on manual press. Long adjustment and composing of single letters into desired text have biggest participation on long working time at gold stamping usage. While at laser scribing is this time shorter thanks to the work in Corel Draw software.

At the conclusion, it is possible to state that increasing of quality of scribing and machined surface, increasing of productivity and economic profit are main priority targets of laser scribing and machining[1–4].

REFERENCES

1. Žídek D.: *Diplomová práce*. FT VUT ve Zlíně, 2005.
2. Halaška P., Manas M.: Laser Cutting Optimization of the Polymeric Plates and Films. In: *42nd Sciece Week Laser Science and Applications*, 2.–4.11.2002, s. 80, University of Aleppo, Syria 2002.
3. Maňková I.: *Progresívné technologie*, Vienala, Košice 2000.
4. Sýkorová L.: *Výzkum mikroobrábění polymerních materialů laserem*. Ediční středisko VŠB-TU, Ostrava 2009.

P-44

FEM MODELLING OF MECHANICAL PROPERTIES OF INJECTION-MOULDED CYLINDRICAL PARTS REINFORCED WITH SHORT FIBRES

OLDŘICH ŠUBA, LIBUŠE SÝKOROVÁ, and ONDŘEJ BÍLEK

Tomas Bata University in Zlín, Faculty of Technology, Department of Production Engineering, T.G.Masaryka 275, 762 72 Zlín, Czech Republic
suba@ft.utb.cz

Abstract

An investigation was carried out through a study of the influence of material anisotropy of the cylindrical plastic parts reinforced by short-fibres, on the stress and deformation. It has been shown that the result of such injection-moulded processes is an anisotropic product, whose mechanical behaviour differs considerably for that of isotropic solids. Some unusual effects of their mechanical properties need to be considered in the course of designing of reinforced plastic parts.

Introduction

Plastic composite parts reinforced by short-fibres are, with increasing frequency, being applied to cases where an emphasis is placed on the level of the utility characteristics value of finished products. The outcome of the resultant distribution and orientation of such short-fibres is, generally speaking, an anisotropic and heterogeneous body whose mechanical behaviour may well be significantly different to that of a conventional understanding of the behaviour of isotropic and homogeneous bodies. A certain weak below of point from the perspective of a potential impairment is represented by thick cylindrical injection-moulded components. With isotropic and unreinforced plastic parts the reason lies in the geometric factor. For anisotropic and heterogeneous structures of injection moulded walls the resultant stress and deformation state due to curving are further affected by material factors.

Problem of layered orthotropic thick cylinder under internal pressure

Let us consider a basic case of a thick cylinder exposed to radial stress. As it is shown in Fig. 1, this can be considered to be a rotationally symmetrical problem. During the moulding process, the fibres may become oriented in a complex manner[1,2]. In the component itself, a characteristic quasi-layered structure is frequently observed. The fibres are oriented in quite different ways according to their location through the thickness of the wall. The polymer melt viscosity and flow rate significantly alter the proportions of the oriented regions. Obviously, for cases of fast injection speeds, the core of the moulding contains fibres mainly aligned perpendicular to the flow direction. Above and below this are regions with the predominant fibre orientation in the flow direction and most of the fibres are lying in planes parallel with the reference plane of the wall.

Selected types of idealized wall structures are shown in Fig. 2. The wall is divided into three layers of identical thicknesses, with different orientation of short fibres 0°, 90°. Case A – in this case it is considered that the short-fibres in skin layers are totally oriented in the direction of the periphery. Vice versa, in case B the fibres in core are totally oriented in the axial direction. The direction of orientation of the short-fibres in a totally oriented structure gives the axis of a monotropic material in given area. The material characteristics in case of linear elasticity are given by the set of elastic constants, making up the appropriate matrix of compliance.

Making up the set of effective elastic constants of a 3D monotropic structure on the basis of experimental measurement is virtually impossible. For this reason, the

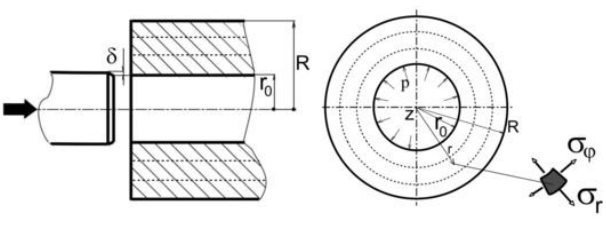

Fig. 1. **Cylindrically symmetric problem of cylindrical thick part**

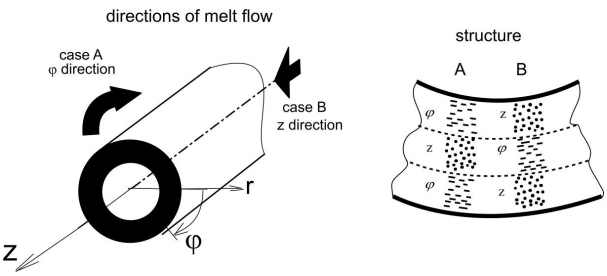

Fig. 2. **Idealized model structures of an injection-moulded cylindrical part**

theoretical prediction of these elastic constants is irreplaceable. We have already mentioned the outcomes of the modelling of the elastic behaviour of short-fibre plastic composites at the micro-mechanical level[2]. Here, we used the results achieved to establish the macro-mechanical model of the cylindrical injection moulded part.

For the purpose of studying the behaviour of highly orthotropic rounded plastic components, we selected an orthotropic case with following values of elastic constants: Modules of the elasticity: E_L = 10560 MPa, E_T = 2340 MPa, Poisson ratios: n_{LT} = 0.367, n_{TT} = 0.576, shear modulus: G_{LT} = 1000 MPa.

Stress state under radial loading

Distributions of stress components of idealised structures of injection wall are compared with stresses of unreinforced polymer, i.e. of isotropic and homogeneous case.

The FEM results are shown in the Fig. 3. Radial displacement of relative value $\delta / r_0 = 0{,}01$ is considered in the inner radius r_0. The values of the maximal peripheral and radial stresses are depicted for cases of structures A, B, and nonfilled that is isotropic and homogenous case. As it follows from the obtained results, peripheral stresses σ_φ reach diverse values dependently on resultant short-fibre structure. These values considerably differ from isotropic and homogenous – nonreinforced case.

In case of structure A, the core – transversal material direction T is strained slightly. However, extensive values of peripheral stress in material direction L imply significant disadvantage of this case. Vice versa, structure B shows low values of peripheral stress σ_φ in the direction L, but levels of stress in material direction T must be taken in account, because the transversal strength of fibrous structures is generally low, obviously at levels of unreinforced polymer.

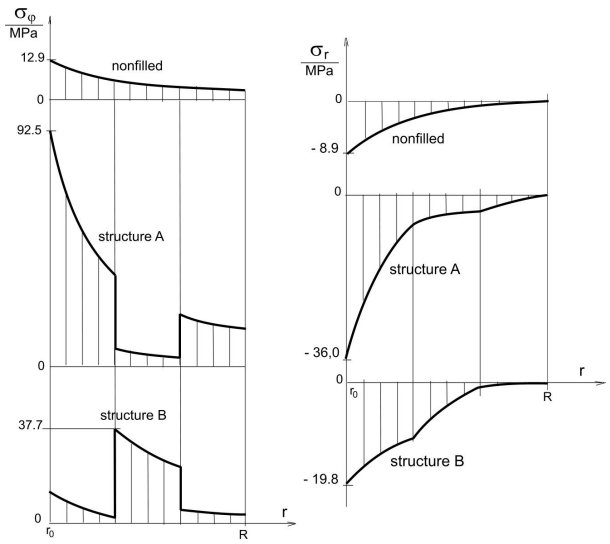

Fig. 3. **Distribution of peripheral stress σ_φ and radial stress σ_r for unreinforced and short-fibre reinforced injection-moulded cylindrical unit.** Curvature ratio R / r_0 =2,5 , relative radial displacement $d / r_0 = 0{,}01$

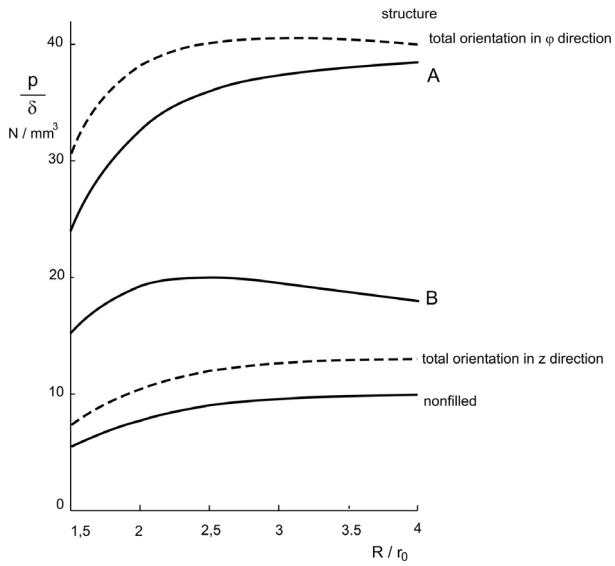

Fig. 4. **Values of radial stiffness versus curvature ratio R / r_0 for unreinforced and short-fibre reinforced injection-moulded cylindrical part.** Relative radial displacement $\delta / r_0 = 0{,}01$.

Similarly, the values of the maximal radial stresses σr are shown in Fig. 3. As has been demonstrated, there is substantial difference in the values of radial stress. However, in both case A and B, stress components σ_r in r_0 fall into the material direction T and thus it is necessary to consider these values of stresses when considering the mechanical behaviour in view of the generally low levels for transverse strength of fibrous materials.

Radial stiffness under radial loading

In order to illustrate the role of the injection-moulded structure in the thick rounded walls like cylindrical bosses, values of radial stiffness of idealised structures of injection wall are compared with unreinforced polymer, i.e. of isotropic and homogeneous case. The results are shown in the Fig. 4. As it follows from the obtained results, radial stiffness reach diverse values dependently on resultant short-fibre structure. These values considerably differ from isotropic and homogenous – nonreinforced case. Further it follows, that values of radial stiffness of cylindrical parts practically do not depend on curvature ratio in ranges of extensive values of R/ r_0.

Conclusions

Load capacity and stiffness of short fibre structures substantially differs from a nonfilled case and thus it is necessary to consider these values when considering the mechanical behaviour of injection moulded parts. The anisotropy and the heterogenity of mechanical properties caused by short-fibre orientation and distribution in melt flow can influence the macromechanical behaviour of injection

moulded parts. Therefore, it is necessary to pay attention to the design of products exposed to higher mechanical loadings. In such a way failures can be reduced at least.

REFERENCES

1. Matsuoka T., Takabatake J.-I., Inoue Y., Takahashi H.: Polym. Eng. Sci. *30*, 957 (1990).
2. Gupta K., Wang K. K.: Polym. Compos. *14*, 367 (1993).
3. Suba O.: In: *Proc. of PPS-16 The Polymer Processing Society, Shanghai, China*. p. 299–300, 2000.

P-45
EFFECT OF PLASTICEZER ON PROPERTIES OF PVA/SO BLENDS

STANISLAVA UHERKOVÁ[a], P. SKALKOVÁ[a], E. JÓNA[a], V. PAVLÍK[b], and I. KOVÁROVÁ[a]

[a] *Faculty of Industrial Technologies, Trenčín University of A. Dubček, I. Krasku 491/30, 020 01 Púchov,* [b] *Institute of Inorganic Chemistry, Slovak Academy of Sciences, Department Of Molten Systems, Dúbravská cesta 9, 945 36 Bratislava 45, Slovak Republic*
uherkova.stanka.u@gmail.com

In recent years, the increasing demand for eco-friendliness packaging and the emphasis of growing environmental awareness stimulated the search for alternative products obtained from renewable sources. One of the many approaches to produce eco-friendly material was to blend biodegradable plastics with natural polymers as reinforcement agent[1]. Polyvinyl alcohol (PVA) is a highly used thermoplastic material that assembles good biocompatible properties and excellent film forming capacity. Due to the characteristics such as easy preparation, chemical resistance, and mechanical properties, the PVA has been used combined with natural polymers in many biomaterial applications[2]. This work deals with preparation of PVA/SO (starch oleate) blends in five different amounts of SO (10, 20, 30, 40, 50 wt.%). As plasticizers was used citric acid (CA) in amounts 10, 25, 35, 50 wt.% in respect of starch oleate. Prepared PVA/SO blends with and without of CA were characterized by FTIR. On prepared blends were studied thermal properties by TG and mechanical properties such as tensile strength, elongation of break.

Experimental part

Materials

Potato starch (approximately 22 % amylose and 80 % amylopectin) was supplied by Spolana Neratovice. The water content was determined by drying the potato starch in a oven at 105 °C until its constant weight and was found to be 10,62 % (w/w). The oleoyl chloride and pyridine were obtained from Aldrich Chemie (Germany). Polyvinyl alcohol – Slovio R16 (16 % – aqueous solution) (PVA) was supplied Fichema Moravians, Czech Republic. Citric acid (CA) (Mw = 192,13 g mol^{-1}) was supplied by Chemapol Praha, Czech Republic.

Esterification of potato starch

Starch oleate (SO, DS = 2,69) was prepared by esterification of starch with oleoyl chloride in the analogous method used to modification of native starch with oleoyl chloride , in pyridine at constant weight ratio 1:3 and at temperature 100 °C and at time 3 h (ref.[3]).

FT-IR spectroscopy

The FT-IR spectra of PVA/SO, PVA/SO/CA films were measured on a FTIR NICOLET 5700 the number of scans 64 cm^{-1} by Company Thermo Electron Corporation.

TG measurements

TG measurements were performed on a Digitalized Derivatograph-Q 1500-D, under air atmosphere, at a heating rate of 10 °C min^{-1} up to 800 °C. The mass loss permits to estimate all the films content and the thermal stability.

Mechanical properties

The mechanical properties were examined according to EN ISO 527-3, 1995 on the unit Hounsfield H20K-W at a speed 5 mm min^{-1}. Five measurements of each samples were tested at 21 °C and the average value of each quantity was reported.

Results and discussion

The spectra of PVA, PVA/SO and PVA/SO/CA films were studied and some spectra are presented in Fig. 1. For each of the films, the spectra of the both sides had the same number of peaks and the positions and relative intensities of these peaks were identicated. In all spectra a peak at 2027, 2160 and 2361 cm^{-1} is due assigned to carbon dioxide in the PVA absorbed from the atmosphere. Peaks due to water in the films occur at 1633 cm^{-1}. The later peak overlaps the peak due to the O–H stretching of hydroxyl groups[4]. Peak at 2922 cm^{-1} it attributes for the CH_2 group, and 1371, 843 and 1084 cm^{-1} are attributed to the C–H stretching, C–H bending and C–O stretching of PVA, respectively. The broad high absorption peak at 3317 cm^{-1} is assumed to arise from the O–H stretching frequencies of PVA and water hydroxyl groups. The band at 1708 cm^{-1} was attributed to the carbonyl functional groups due to residual acetate groups remaining after the manufacture of PVA from hydrolysis of polyvinyl acetate or oxidation during manufacturing and processing[4]. In the spectrum PVA and PVA/SO films there are new band peaks at 1636 cm^{-1}, which are attributed to C=C band stretching groups of oleate. FT-IR spectra of PVA/SO films show characteristic band at 1738 cm^{-1} where their intensity increases with increasing content of SO than the through conjugation C=C bonds. Peaks at the value 2922 cm^{-1} and 2871 cm^{-1} are characteristic for CH_2 groups and their intensity increases with increasing content SO.

The FT-IR spectrum of prepared PVA/SO/CA films

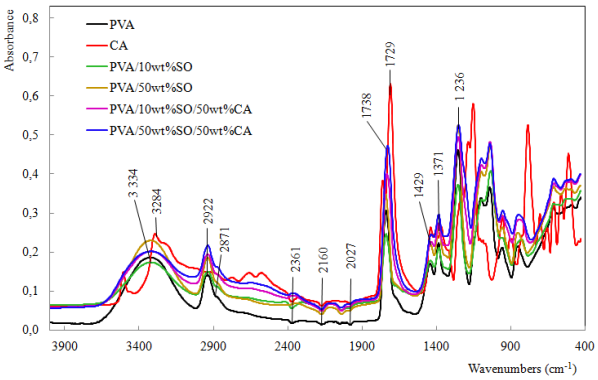

Fig. 1. **FT-IR spectra of PVA and PVA/SO films with different amounts of SO and plasticizer CA**

(Fig. 1) shows bands at the value 2922 cm^{-1} and 2871 cm^{-1} are characteristic for CH_2 groups and their intensity increases with increasing content SO and CA. In spektra of citric acid band around 3284 cm^{-1} is assigned to the stretching vibration of the hydroxyl groups.

The intensity band OH groups of prepared films increased and the maximum shifts to higher wave numbers. The effects of CA on the FT-IR spectra of PVA, PVA/SO and PVA/SO/CA films are shown in Fig. 1. In the spectrum citric acid band at 1729 cm^{-1} it atributed C=C group. By increasing the amount of citric acid in PVA/SO films increases the intensity of this band. Probably this phenomenon illustrates that the esterification occurred more easily between the SO and CA than that between PVA and SO acordink as in the work[5].

TG curves pure PVA showed a two-step decomposition. The first step began around 80 °C, and the second one began around 225 °C. The final temperature of the decomposition was around 565 °C. TG profile of the PVA/SO films presents three degrading areas. The first in the range from 80 °C to 225 °C is related to desorption of water, resulting in 12 % of mass loss in this interval. The second mass loss, observed from 320 °C to 427 °C, is probably associated to degrading of PVA chains, representing 66 % of mass loss. In the last degrading areas, from 510 °C to 552 °C, a mass loss of 12 % was observed is related to SO. Important observation can be extracted from TG analysis and increasing the SO content in the PVA/SO film will increase thermal stability of the blended film. The addition of CA obviously reduced the mass loss rate and increased the residual mass percentage at 600 ° C. After of CA content was added, the shape of the TG curve of PVA/SO/CA changed as compared to that of CA. The films showed a three-step of decomposition. The first step was attributed to the elimination of water from films. The second step was same as that of PVA. The third step was attributed to the SO and cross-linked CA component. The TG curves of PVA/SO/CA films showed a three-step decomposition: 80–165 °C, 318–427 °C, 492–552 °C, which is similar to the classical TG curve of the PVA and to the PVA/SO films.

Tensile strength of PVA/10 wt.% SO film compared to tensile strength of pure PVA. With increasing content of SO in PVA films, tensile strength increases. The tensile strength of plasticized PVA films with amounts of SO out of 30 wt.% increases. In addition, PVA film plasticized with 10 wt.% CA, where the tensile strength decreases with increasing amount of SO. CA has a negative effect on the tensile strength of prepared PVA/SO films. The mechanical properties are not only related with the cross linker but are also related with the plasticizer. The cross linker and the plasticizer always have the contrary effects on the tensile properties. Generally, the tensile strength increased and the elongation at break decreased as the percentage of cross linker increased. The results are opposite when the plasticizers increased. The CA acted both as the cross linker and the plasticizer in composites. So that different functions of CA would be exhibited when different amounts of CA were added[6]. The residual CA in the blends played a role as the plasticizer, which reduced the interactions among the macromolecules, which resulted in the decrease of the tensile strength and increase of the elongation at break. Elongation at break of PVA films without plasticizer (CA) with increasing amount of SO slightly increasing. Elongation at break of PVA films containing CA (10, 25 wt.%) is about the same course as the elongation at break unplasticized films. Elongation at break of PVA film with 50 wt.% CA with amount of SO out of 30 wt.% increased. It reaches a maximum value of 31 wt.%. It can be concluded that the high content of plasticizer (50 wt.% CA) has a positive effect on the elongation break.

Conclusion

The PVA/SO films were prepared with and without of plasticizer citric acid. Evidence for the modification of the films has been obtained from by means several techniques including FT-IR, TGA and mechanical properties. In the structural changes gave rise to a series of property changes. The thermal stability improved as function of cross-linking and it improved molecular interactions. The mass loss is improved compared with pure PVA. The tensile strength in the majority of samples reduced but sampling PVA/40 wt.% SO (85,7 MPa) and PVA/40 wt.% SO/25 wt.% CA (92,5 MPa) in comparison with the pure PVA (84,9 MPa). Elongation at break is reduced most samples except samples PVA/10 wt.% SO/35 wt.% CA (21,23 %), PVA/10 wt.% SO/50 wt.% CA% (50,4 %), PVA/40 wt.% SO SO/50 wt.% (11,6 %) and % PVA/50 wt.% SO/50 wt.% CA (31 %) in comparison with the pure PVA (3,6 %). This was caused by the plasticizing effect of the CA in the blend.

REFERENCES

1. Lopez-Rubio A., Gavara R., Lagaron J. M.: Trends Food Sci. Technol. *17*, 567 (2006).
2. Srinivasa P. C., Ramesh M. N., Kumar K. R., Tharanathan R. N.: Carbohydr. Polym. *53*, 431 (2003).
3. Abburto J., Thiebaud S., Alric I., Borredon E., Bikiaris D., Prinos J., Panayiotou C.: Carbohydr. Polym. *34*, 101 (1997).
4. Jayasekara R., Harding I., Bowater I., Christie G. B. Y., Lonergan G. T.: Palymer Testing *23*, 17 (2004).
5. Rui S., Jingliang B., Zizheng Z., Aichen Z., Dafu C., Xinhua Z., Liqun Z., Wei T.: Carbohydr. Polym. *74*, 763

(2008).
6. Sreedhar B., Sairam M., Chattopadhyay D. K., Syamala Rathnam P. A., Mohan Rao D. V.: J. Appl. Polymer Sci. *96*, 1313 (2005).

P-46
CONDUCTIVE MAGNETOPOLYMER COMPOSITES WITH FERROSILICON FILLER

MARIANA UŠÁKOVÁ*[a], JANA REKOŠOVÁ[b], ELEMÍR UŠÁK[a], RASTISLAV DOSOUDIL[a], and IVAN HUDEC[b]

[a] Slovak University of Technology in Bratislava, Faculty of Electrical Engineering and Information Technology Ilkovičova 3, 812 19 Bratislava, [b] Slovak University of Technology in Bratislava, Faculty of Chemical and Food Technology, Department of Plastic and Rubber, Radlinského 9, 812 37, Bratislava, Slovak Republic
mariana.usakova@stuba.sk

The magneto-polymer composites comprise the magnetic fillers incorporated into the non-magnetic polymer matrix. These materials attract increasing interest in electrical engineering applications especially thanks to the simplicity of fabrication process. The polymer magnetic composites with conductive magnetic filler are also characterised by good electromagnetic properties. In comparison to spinel ferrite/ polymer absorbers, the composites with conductive magnetic filler exhibit better electromagnetic wave (EM-wave) absorbing properties, such as lower matching thickness and wider EM-wave absorbing bandwidth[1,2].

The purpose of this work was the study of magnetic and physical-mechanical properties of magneto-polymer composite materials. Vestamid® L2122 polyamide was used in the investigated materials as the non-magnetic polymer matrix. Commercially manufactured ferrosilicon powder FeSi15 C-60 was used as the magnetic filler. The magneto-polymer composite samples with filler contents varied from 0 to 60 vol.% were prepared by mixing the magnetic filler and polymer matrix in the laboratory mixer at 190 °C.

Structural characteristics, such as size, shape and distribution of used filler were investigated by means of laser particle distribution analyser. Physical-mechanical properties of prepared composites were measured in accordance with valid technical standards on the double side blade specimens (width 6.4 mm, length 100 mm, thickness 2 mm). Static magnetic properties of prepared samples represented by initial permeability were measured by means of customised software-controlled experimental equipment built-up from commercially available instruments. Dynamic magnetic properties, such as e.g. the frequency dependencies of real (μ') and imaginary (μ'') parts of the complex permeability of the composites were obtained by means of impedance spectroscopy (coaxial S-parameter method) in the frequency range from 10 MHz to 6.5 GHz. The measured composite samples were prepared in the form of toroids with an outer diameter of 8 mm, an inner diameter of 3.5 mm and a height of 2 mm. The conductive magnetic ferrosilicon filler with the content of 82.5 % Fe, 15.0 % Si and small amounts of C, Al,

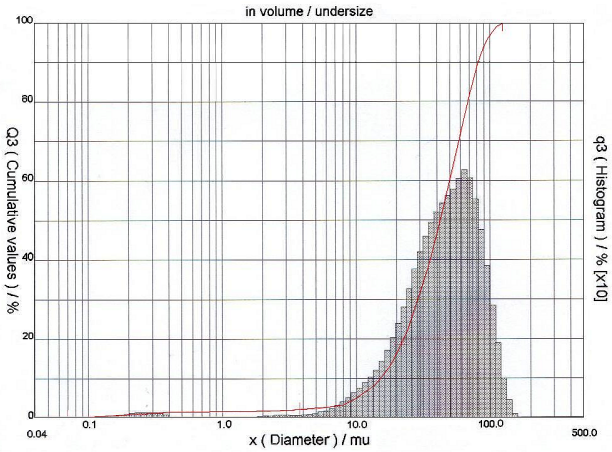

Fig. 1. **Particle size distribution of ferrosilicon filler**

Mn and Cr (≤ 1 %) consists of randomly shaped particles with diameter less than 100 µm. The size of FeSi particles was verified by laser particle size distribution (Fig. 1)[2].

The magnetic filler in polymer matrix clearly influences physical-mechanical and magnetic properties of composite samples. The dependence of the tensile strength value as a function of ferrosilicon contents in prepared magneto-polymers initially shows rapid fall - the tensile strength value decreased about 48 % for the sample with ferrosilicon concentration 10 vol.% in comparison with tensile strength value of pure polymer sample. Further increasing of magnetic filler content caused only slight decrease of tensile strength value oscillating about 20 MPa (Fig. 2, solid line, open circles). The influence of ferrosilicon filler on the Young's modulus of composite samples is even more significant (see Fig. 2, dashed line, closed circles), The values of Young's modulus increase with magnetic filler content; for the maximum concentration (60 vol.%) it was about 7 times higher than for pure polymer.

The dependencies of initial permeability (μ_i) upon filler concentration measured at the frequency of 50 Hz (quasi-

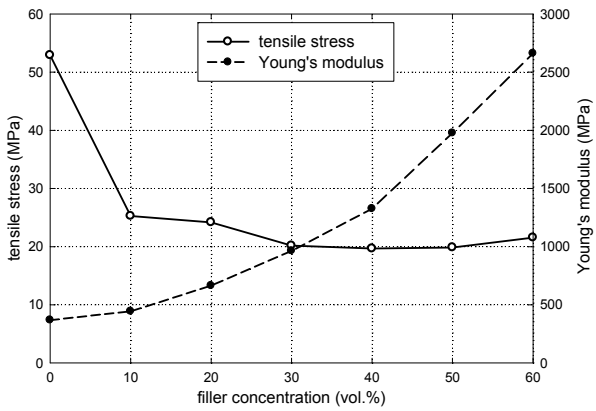

Fig. 2. **Dependence of the tensile strength and the Young's modulus value on ferrosilicon content of magneto-composites**

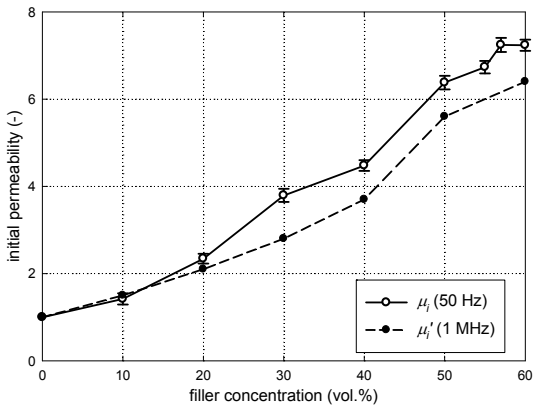

Fig. 3. **Dependence of initial permeability on ferrosilicon content of magneto-composites**

static for these materials) as well as the real component of complex permeability at constant frequency of 1 MHz (μ_i') are displayed in Fig. 3. One can see almost linear increase of the permeability values with the increase of ferrosilicon amount.

Note that the real part μ_i' (Fig. 3; dashed line, closed circles) gives slightly less values than quasi-static (50 Hz) initial permeability μ_i (Fig. 3; solid line, open circles). This can easily be explained by the influence of the eddy currents, since FeSi is a metallic (thus, electrically conductive) alloy.

The frequency dependencies of real and imaginary parts of complex permeability for the prepared composite samples are shown in Fig. 4. The values of μ_i' shown in Fig. 3 originate from Fig. 4a. We can observe the typical relaxation type of frequency dispersion of permeability with only one dispersion range. The real component of permeability for all the composites nearly monotonically decreased meanwhile the imaginary part of permeability increased with frequency and reached the maximum value at the resonant frequency f_r, (see also Table I). On the other hand, the resonant frequency f_r, raises from 0.32 GHz for 60 vol.% composite sample to over 3 GHz for 10 vol.% one. This behaviour is the direct consequence of two phenomena, namely the domain wall resonance and the natural ferromagnetic resonance[3,4]. The domain walls follow the high-frequency ac electromagnetic field up to about 10^8 Hz, over this value they cannot follow the changes of exciting field and their contribution to permeability starts to decrease. As a result, the measured

Table I
Real component of complex permeability at the lowest frequency μ_i' and resonant frequency f_r, for FeSi-PAD composites

Filler content (vol.%)	10	20	30	40	50	60
μ_i' (–)	1.5	2.1	2.8	3.7	5.6	6.4
f_r (GHz)	>3	2.83	1.27	0.72	0.38	0.32

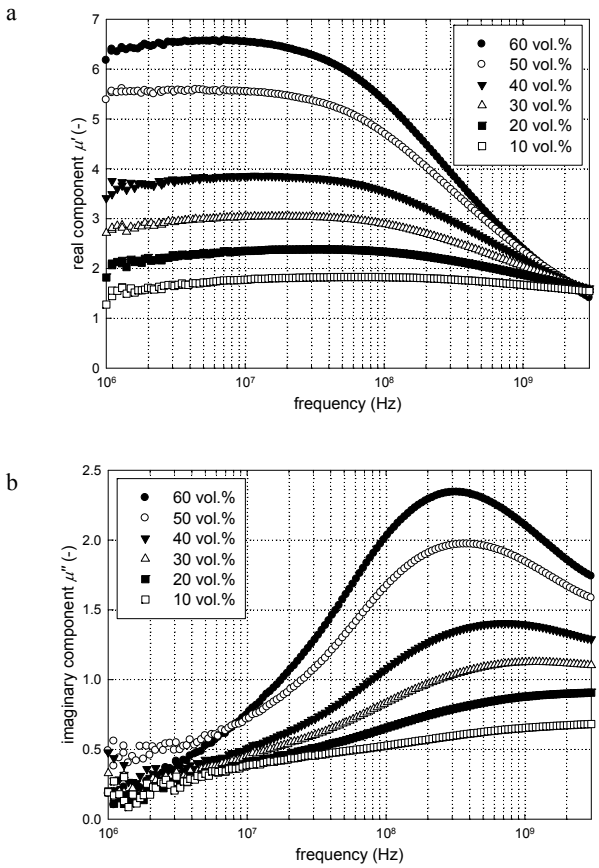

Fig. 4. **Frequency dependences of a) real and b) imaginary parts of complex permeability for FeSi-PAD composites with various filler contents**

dispersion of permeability is mainly caused by the natural ferromagnetic resonance. The decrease of μ_i' and increase of f_r with reduced FeSi filler content in composite materials is associated with the origin of the demagnetising field formed in filler particles dispersed in polymer matrix[3].

The experiments confirmed the impact of ferrosilicon FeSi15 C-60 powder filler content on both the physical-mechanical properties as well as magnetic properties of the composites.

This work was supported by the Slovak Research and Development Agency under the contract No. APVV-0062-11 and by the Scientific Grant Agency of the Ministry of Education, Science, Research and Sport of the Slovak Republic and the Slovak Academy of Sciences (VEGA), projects No. VG-1/1163/12 and VG-1/1325/12.

REFERENCES

1. Yi Z., Shuhua Q., Fan Z., Yongqing Y., Guochen D.: Appl. Surf. Sci. *258*, 732 (2011).
2. Dosoudil R., Ušáková M., Sláma J.: Chem. Listy *105*, 429 (2011).

3. Dosoudil R., Ušáková M., Franek J., Sláma J., Grusková A.: IEEE Trans. Magn. *46*, 436 (2010).
4. Dosoudil R., Franek J., Sláma J., Ušáková M., Grusková A.: IEEE Trans. Magn. *48*, 1524 (2012).

P-47
MODIFICATION OF PUR DISPERSIONS IN THE ADHESIVES FOR 3D BONDING IN THE FURNITURE INDUSTRY

VLADIMÍR VANKO[a], IGOR NOVÁK[b], JOZEF PREŤO[a], and JÁN HRONKOVIČ[a]

[a] *Vipo Partizanske,* [b] *Polymer Institute of the Slovak Academy of Sciences, Dúbravská cesta 9, 845 41 Bratislava 45, Slovakia*
vvanko@stonline.sk

Abstract

The aim of the work was the study of modification PUR dispersions used in adhesives for 3D bonding of high glossy foils in the furniture industry. The hydrophobization additives were used in order to improve the wetting of bonding substrate – middle density fiberboard (MDF). The influence of additives was examined by the measurement of contact angle, shear strength of adhesive joint, tensile strength at break of adhesives films and surface quality of adhesive joint. In relation to modification of PUR dispersion was examined also the influence of modification MDF surface by the barrier plasma. The experiment showed that the addition of hydrophobization additives improves the wetting properties of PUR dispersions and has positive effect on surface quality of adhesive joint.

Introduction

Polyurethane dispersions generally consist of urethane urea polymers dispersed in water in preference based on aliphatic polyisocyanates and therefore offer good resistance to discoloration[1]. Heat-activated adhesives based on polyurethane dispersions have become established for joining processes in which synthetic materials need to be adhesively bonded and are gradually displacing conventional solvent-based adhesives[2]. Examples include laminating PVC foils on MDF sheets. Usually polyester PUR dispersions are preferred for bonding soft PVC due to their good plasticizer resistance. For 3-D laminating PVC foils on MDF sheets the polyurethane dispersion adhesives can be applied either as two-component materials, i.e. in combination with a hydrophilically modified isocyanate, or in the form of a latent-reactive dispersion with a surface-deactivated solid isocyanate which are applied by spraying on the surface of profiled MDF[3] .When high glossy foils are used the problem of rough surface is observed, caused by poor quality adhesive spread or eventually by next processes of his drying, pressing and curing. In generally the right formulated PUR dispersion adhesive suitable for the bonding of high glossy foils should meet two basic requirements of good wetting and flowing properties as well as the lower reactivation temperature of 50–55 °C. The lower the press reactivation temperature, the less the elasticity of the foil and hence the less risk of the soft foil telegraphing an uneven surface of the adhesive coated MDF. The wetting properties of examined system are possible to change not only by the modification of adhesive but also by the treatment of bonded substrates. When the plasma treatment is used the significant changes on the surface are observed[4]. Among numerous kinds of electric discharge plasmas, coplanar surface barrier plasma at atmospheric pressure and/or radio-frequency volume plasma at reduced pressure are currently the most promising methods of surface modification, and are considered as the 'green' ecologically friendly modification method[5].

Because the surface of evaluated MDF is non-polar – hydrophobic, when the polar component of surface energy MDF is significantly lower than polar component of surface energy of films prepared from Dispercoll U 53 (ref.[6]), we studied in our work two kinds of modifications: The addition of oleic acid which is non-polar to polyurethane dispersion in order to reach the better wetting properties on the MDF as a basic presumption for smoother surfaces of adhesive joints and also was studied the treatment of MDF sheets by the coplanar barrier plasma and its influence on wetting and bonding characteristics.

Experimental

In this study was used the commercial polyurethane dispersion Dispercoll U 53 produced by Bayer, Germany. The properties of Dispercoll U 53 are described in the Table I. As a hydrophobization additive was used oleic acid in pure quality. The content of oleic acid in PUR dispersion was given as weight % calculated on polymer content of PUR dispersion. MDF was type Antine, density 800 kg m^{-3}, produced by Bipan, Italy, PVC foil was Darkar HG, thickness 0, 5 mm produced by Riken Technos, Japan.

The wetting properties were evaluated by measurement of contact angles with selected testing liquids set using SEE (Surface Energy Evaluation) device completed with a web camera (Advex, Czech Republic) and necessary PC software. The adhesive joints for measurement of shear strength were prepared by pressing at the temperature 60 °C on the hydraulic press Fontijne SR 100 and evaluated by Instron 4301. The dispersion spread was done by brush only on MDF, 30 minutes drying. Adhesives films for the measurement of tensile strength were prepared by spraying in several layers on inert board. The adhesive joints for evaluation of surface

Table I
The basic properties of used polyurethane dispersion

Product	Polymer content [%]	Viscosity [mPa s]	pH	Density [g cm^{-3}]	Minimum activation temperature [°C]
Disper-coll U 53	40±1	50–600	7.5	approx. 1.07	45–55

quality were prepared by spraying dispersions on MDF; adhesive coating was approx. 40 g m^{-2}, dried 30 minutes and pressed on vacuum membrane press in the Decodom Ltd. Topoľčany in standard technology conditions. The surface quality of adhesive joints was evaluated using Wave scan II device from BYK Instruments, as a value of waviness with the length 2–15 mm referred to as longwave. They were evaluated in horizontal and vertical direction respective the direction of spraying. The content of longwave is decisive factor for evaluation of surface quality regarding to sensitivity of human eye from the observing distance over 50 cm (ref.[7]).

Plasma modification was implemented in static conditions by diffuse coplanar barrier surface discharge (DCSBD) plasma technology of laboratory scale at atmospheric pressure and room temperature.

Results and discussion

The contact angles of modified Dispercoll U 53 by the adittion of oleic acid on MDF, tensile strength of adhesive films and shear strength of adhesive joints are shown in Table I. The addition of oleic acid causes changes in wetting properties of Dispercoll U 53.The contact angles of modified Dispercoll U 53 were significantly decreased.As beter is wetting the higher shear strength of adhesive joint was expected. The higher shear strength was reached only up to addition of 2 weight % oleic acid and next addition of oleic acid caused the decrease of shear strength. It can be related to potential incompatibility of oleic acid in Dispercoll at higher concentrations resulting in worse adhesion and cohesion properties. The cohesion of PUR films was decreased and the shear strength well correlates to tensile strength of adhesive films.

Table II
Shear strength of adhesive joints, contact angles and tensile strength of films modified Dispercoll U 53

Content of oleic acid [%]	Shear strength of adhesive joint [MPa]	Contact angle [deg]	Tensile strength at break [MPa]
0	12,0	101,4	19,6
1	12,3	91,9	19,6
2	12,5	86,3	19,5
3	10,9	83,6	19,0
4	8,5	80,7	17,2
5	7,9	77,1	12,0

The influence of addition of oleic acid on the surface quality of adhesive joints is shown in Fig. 1.The higher is content of oleic acid the lower value of longwave in both direction we reached. The lower value of longwave means the smoother surface of adhesive joints.

The contact angles modified Dispercoll U 53 with oleic acid on treated surface MDF by plasma are shown in the Fig. 2. After treatment of surface MDF by plasma the contact angles modified Dispercoll U 53 were significantly decreased. The addition of non-polar oleic acid causes better wetting although the treatment by plasma causes higher polarity of surface MDF[6].

The shear strengths of adhesive joints given in Fig. 3 are significantly affected by the exposure time of treatment surface MDF by plasma and addition of oleic acid. The values of shear strengths increase with the exposure time only when unmodified Dispercoll U 53 is used. The addition of oleic acid causes the decrease of shear strengths. It can be explained by different effect both types of modifications. With longer exposure time of plasma treatment is surface of MDF more polar and with higher content of oleic acid is dried PUR film more non-polar.

Conclusion

The addition of oleic acid to polyurethane dispersion improves the wetting properties of PUR dispersion and has

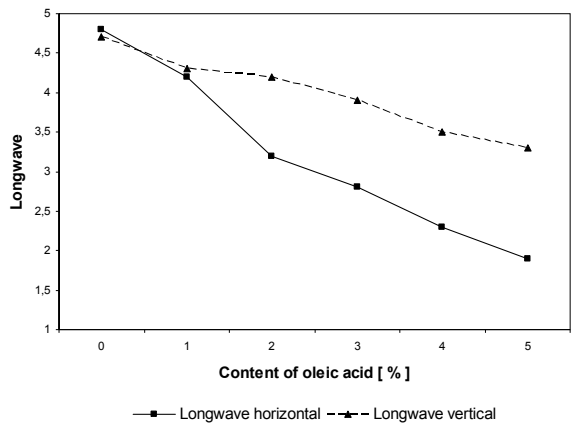

Fig. 1. **Dependency of longwave surface of adhesive joints on content of oleic acid**

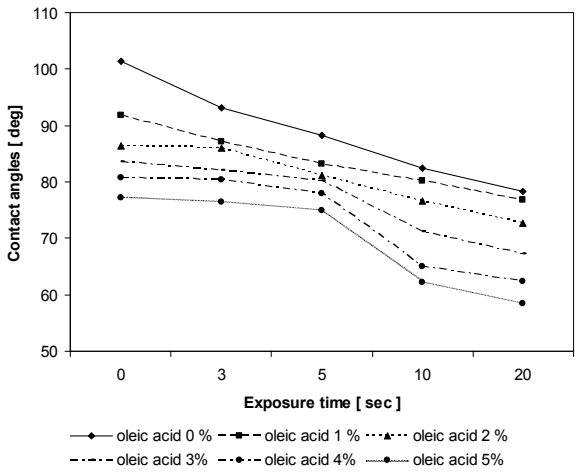

Fig. 2. **The contact angles modified Dispercoll U 53 by oleic acid as function of exposure time of plasma treatment surface MDF**

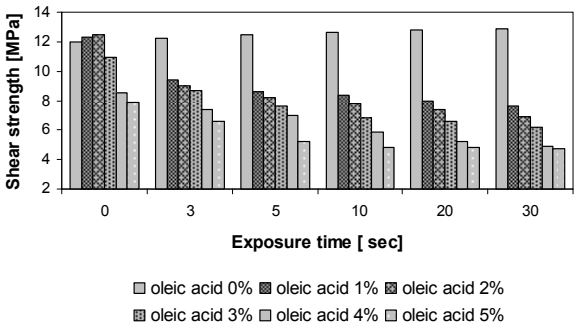

Fig. 3. **Dependency of shear strength of adhesive joint on the content added oleic acid and exposure time of plasma treatment surface of MDF**

positive effect on surface quality of adhesive joint and also improves the shear strengths up to 2 weight % of oleic acid. The modification of PUR dispersion by oleic acid is the potential way how to formulate the adhesives for 3-D bonding of glossy foils in furniture industry.

When the plasma treatment of surface MDF was applied the significant decrease of contact angles and shear strengths were observed when the oleic acid was added to PUR dispersion. Using the both kind of modifications together is not the right way how to modify and apply the PUR dispersions.

This work was prepared as part of the project „Application of Knowledge-based Methods in Designing Manufacturing Systems and Materials“, project No. MESRSSR 3933/2010-11.

REFERENCES

1. Bodo Müller, Walter Rath: „Formulating adhesives a sealants“, 2010, p. 67 – 71.
2. D. Dieterich: Angewandte Makromolekulare Chemie *98*, 133 (1981).
3. Jörg Büchner, Wolfgang Henning: “Latent – reactive and storable“, adhesion ADHESIVES & SEALANTS 9/2007, p. 4–8.
4. Novák I., Popelka A., Vanko V., Chodák I., Preťo J.: “Modification of wood by low-temperature atmospheric discharge plasma”, Annals of Warsaw University of Life Sciences – SGGW Forestry and Wood Technology No 75, 2011: 135–141
5. Kiguchi M.: Surface modification and activation of wood. In: Hon D. N. (ed.), *Chemical modification of lignocellulosic materials*. Marcel Dekker, New York 1996.
6. Novák I., Vanko V., Preťo J, Chodák I.: ”Povrchové a adhézne vlastnosti substrátov v spoji drevotriesková doska –PVC fólia lepenom polyuretánovým adhezívom”, *63. Zjazd chemikov,5.–9.9.2011,Tatranske Matliare*
7. Catalogue of BYK products for 2010 – 2011. p 33–47.

P-48

APPLICATION OF CORN STARCH AS A FILLER IN RUBBER BLENDS

PETRA VÁŇOVÁ[a], IVAN HUDEC[a]*, and ALENA KŇAZEOVÁ[b]

[a] *Slovak University of Bratislava, Faculty of Chemical and Food Technology, Radlinského 9, 812 37 Bratislava,*
[b] *VEGUM a.s., Gumárenská 337, 972 23 Dolné Vestenice, Slovakia*
petra.vanova@stuba.sk

In the last periods, the major environmental problem relating to increasing amount of waste rubber production has become still more actual. The rubber waste remains in landfills many years without a change of its volume. Sources of rubber compounds are often non-renewable and their exhaustion loses the ability to manufacture these products. Therefore, in the recent years, the producers of rubber have been searching for new renewable sources, environmentally safe that might be able to support decomposition of rubber products, and thus they could contribute to reducing of waste rubber.

This work is focused on the application of corn starch as a filler for elastomeric composites based on EPDM. There was observed the influence of natural filler on the curing process and physical-mechanical properties of EPDM blends. The main goal was to find suitable amount of used corn starch in combinations with other additives of rubber compounds in order to support biodegrability and to reduce the cost of the final products. The corn starch was applied in natural form, and also after subsequent drying. The results indicate the possibility of application of corn starch in rubber blends, but in many cases it is necessary to modify corn starch before it is used.

Introduction

Starch is a dominant carbohydrate that represents reserve material of higher plants. Starch consists of two basic types of α-D-glucose homopolymers, namely amylose and amylopectin. Amylose is a linear molecule composed of anhydroglucose units connected through (1/4)-α-linkages and with a few (1/6)-α-linkages, too. Amylopectin is a much larger molecule with very branched structure built from about 95% (1/4)-α- and 5 % (1/6)-α-linkages[1]. The ratio between amylose and amylopectin varies depending on the starch source. In normal starches, amylose constitutes about 15–30 % of total starch.

The size and shape of starch granules vary in different plant species. Starch granules have a semi-crystalline structure with a typical crystallinity around 15–45 % (ref.[1]). Starch is a plentiful, biodegradable, naturally renewable, environmentally friendly, and inexpensive nature polymer[2]. Starch characteristics have an influence on the properties of final products, into which they are added, such as viscosity, moisture retention, gel formation and product homogeneity.

A considerable interest has been focused on finding new applications for this biopolymer in food and also non-food industry, for instance as low-calorie substituent,

biodegradable packaging materials, thin films and thermoplastic materials with improved thermal and mechanical properties[3]. Native starch does not have high thermal stability and tends to form agglomerates and that's the reason why it often undergoes the surface modification.

Experimental

Ethylene propylene diene rubber EPDM (DUTRAL TER 4049 Polimeri, Italy), was compounded with various amount of corn starch (in native and dried form) in order to prepare rubber composites. The content of processing additives, fillers (carbon black N550 and kaolin) and components of sulfur curing system was kept constant in all experiments. Corn starch (the trade name Meritena 100) with moisture content 11 % and pH 6.7 was supplied by AMYLUM SLOVAKIA, Boleráz. The content of corn starch in rubber blends varied from 0 to 40 phr.

The methods and procedures

The rubber compounds were prepared in laboratory mixer Brabender in two mixing steps. In the first step, the rubber, the processing additives and the fillers were mixed together. In the second step, the curing system was introduced.

The curing characteristics of prepared materials were determined from the corresponding curing isotherms measured by rheometer Monsanto R100 at 150 °C. The curing process of rubber compounds was performed in hydraulic press at 150 °C under a pressure of 15–17 MPa for the optimum cure time.

The tensile properties of cured rubber compounds were measured by using ZWICK ROELL/Z 2.5 appliance at cross-head speed of 500 mm min^{-1} at laboratory temperature in accordance with the valid technical standards. The hardness Shore A of vulcanizates was measured.

Results and discussion

As seen in Fig. 1, by incorporation of 10, 20 and 30 phr corn starch in native form into rubber compounds the optimum cure time t_{c90} decreased in comparison with t_{c90} of the sample which content only carbon black and kaolin, used as reference. The sample with 40 phr of applied filler required the longest time essential for curing process. The optimum cure time of rubber compounds filled with dried corn starch was found to be much longer in comparison with the previous systems.

The values of physical-mechanical properties of prepared composites are illustrated in Figs. 2–4. The tensile strength at break of vulcanizates showed the decreasing tendency with increasing amount of applied corn starch as shown in Fig. 2.

The differences in the values of tensile strength at break of vulcanizates in dependence on the type of filler were different. At lower filler contents (10, 20 phr), higher values of tensile strength at break were spotted in case of vulcanizates with corn starch applied in native form. Higher values of tensile strength at break of samples with higher filler contents (30, 40 phr) were reached by incorporation of corn starch in dried form.

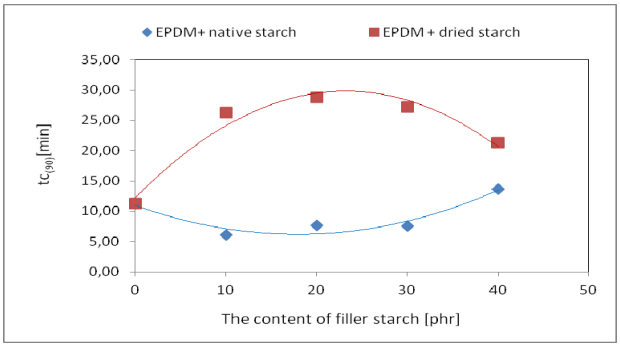

Fig. 1. **Influence of corn starch content on optimum cure time $t_{c(90)}$ of rubber blends based on EPDM**

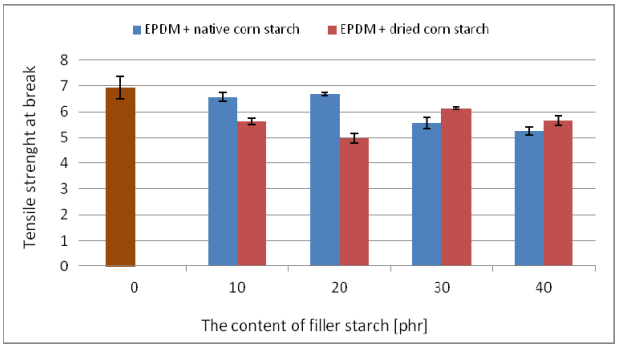

Fig. 2. **Influence of corn starch content on tensile strength at break of vulcanizates based on EPDM**

From Fig. 3 it evident, that the elongation at break of vulcanizates with corn starch in native form was kept almost unchanged up to 20 phr of filler incorporated. Then sharp decrease of elongation at break values was recorded at higher corn starch contents. In case of samples with dried corn starch, rapid decrease of elonagtion at break was possible to see by application of 10 phr filler. The elongation at break values of samples with higher filler contents were similar to those of equivalent samples with corn starch in native form.

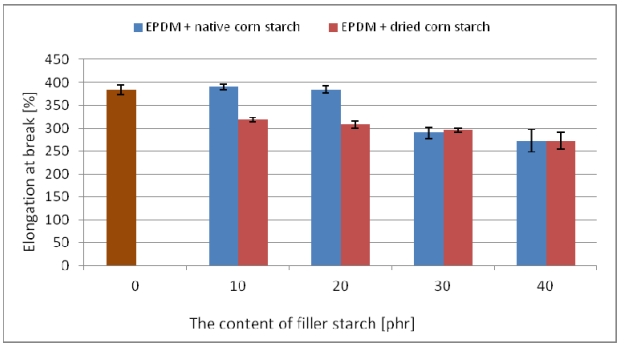

Fig. 3. **Influence of corn starch content on elongation at break of vulcanizates based on EPDM**

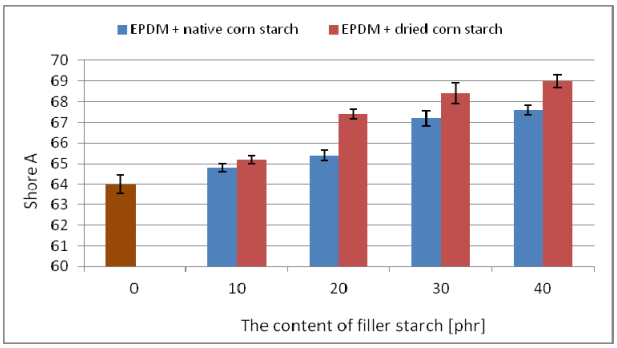

Fig. 4. **Influence of corn starch content on hardness of vulcanizates based on EPDM**

The hardness of vulcanizates (Fig. 4) increased with increasing amount of corn starch, as the hardness of corn starch particles is higher than the hardness of the rubber matrix. The highest values of hardness were reached by applying of corn starch in dried form.

Conclusion

The results achieved by the study revealed that the presence of corn starch in rubber compounds influences the curing process and also the physical-mechanical properties of rubber compounds. The decrease of tensile strength at break and elongation at break with increasing content of corn starch was recorded. The reason might be attributed to the structure of natural filler and the presence of hydroxyl groups on the surface of corn starch particles, which tend to form intra- and intermolecular hydrogen bonds. This leads to the forming of aggregates and agglomerates of filler particles in the rubber matrix, what to a large extent contribute to the deterioration of observed properties. Weak mutual interactions and adhesion between the particles of corn starch and the rubber matrix could be the next reason why corn starch does not act as a reinforcing filler in rubber matrix. Seeing that the incorporation of examined type of corn starch into the rubber compounds caused the decrease of observed properties of equivalent vulcanizates, the utilization of such materials is so far estimated for applications, which are not subjected to the excessive dynamic-mechanical strain. On the other hand, the increase of hardness of prepared systems in dependence of corn starch contents suggest that such materials could be possibly used in applications required higher hardness and stiffness of final products. For broader utilization of such systems, the efficient methods of corn starch modifications should be developed, in order to improve the compatibility and adhesion between the rubber matrix and the particles of corn starch.

REFERENCES

1. Chung Y.-L., Lai H.-M.: Carbohydr. Polym. *63*, 527 (2006).
2. Ren L.-L., Jiang M., Wang L., Zhou J., Tonga J.: Carbohydr. Polym. *87*, 1874 (2012).
3. Kaur B., Ariffin F., Bhat R., Karim A. A.: Food Hydrocolloids *26*, 398 (2012).

P-49

THE INFLUENCE OF DYEING TIME AND TEMPERATURE FOR THE DYEABILITY OF UNTREATED AND PLASMA TREATED COTTON FABRICS

PETRONELA VENCELOVÁ*, ANNA UJHELYIOVÁ, MONIKA BOTOŠOVÁ, MILAN MIKULA, ĽUBA HORBANOVÁ, and MARCELA HRICOVÁ

Slovak University of Technology in Bratislava, FCHFT, Institute of Polymer Materials, Radlinského 9, 812 37 Bratislava, Slovak Republic
petronela.vencelova@stuba.sk

Introduction

Plasma is a partially ionized gas, containing a mixture of electrons, positive and negative ions, radicals, and various excited molecules. It might be regarded as a "fourth state of matter"[1,2]. Historically, plasmas could be produced only at high temperatures or in vacuums; however, recent breakthroughs, in plasma physics have allowed development of plasma at room temperature and atmospheric pressure, so-called non-thermal or (cold or low temperature) atmospheric plasma[1].

Atmospheric plasma has many advantages. It can be generated under atmospheric conditions and requires no vacuum systems and therefore can be applied on-line for textiles[3,4]. The species that participate in plasma reactions (excited atoms, free radicals and metastable particles, electrons and ions) can interact either physically or chemically with the substrate[3]. Exposure of natural fabrics to a plasma environment can produce more reactive surfaces.

This type of plasma is used in surface modification. It is a very helpful technique where surface chemical modification is required. Plasma treatment modifies surfaces without affecting the characteristics of the bulk. Consequently, plasma processes have found a wide range of very important technological applications of surface energetic to improve adhesion strength cleaning, coating[2]. Plasma surface modification does not require the use of water and chemicals, resulting in a more economical and ecological process[4].

In this paper the influence of dyeing time and temperature for dyeing of untreated and plasma treated cotton fabrics was investigated. There was evaluated % of exhaustion after dyeing. FTIR was used for analysing the cotton fabrics after dyeing and after dyeing the values of rubbing fastness were determined.

Experimental

Material used

The woven textile fabrics from cotton were used as a substrate for the treatment of low temperature plasma and subsequently were dyed.

Methods used

The surface of cotton textiles were activated by low temperature plasma generated discharged at the atmospheric

pressure at 350 W for 3 seconds. There was used different ageing time (AT) 10, 20 and 30 minutes.

Then there was measured % of exhaustion dyeing (ED) of cotton untreated and treated fabrics. Samples were dyed by classical exhaustion dyeing from bath.

The equipment AHIBA ↑↓ AG CH 4127 Bisfelden (Switzerland), type G6 RTC (4.4 kW) was used for the dyeing of cotton materials by classical exhaustion method from bath. Conditions for dyeing were followed:
As the dye was used – Bezaktiv Rot, concentration of dye – 2 % o.w.f., concentration of auxiliary agents – 20 g l^{-1} Na_2CO_3 and 75 g l^{-1} NaCl, dyeing time was 30 and 60 minutes, dyeing temperatures were 60 and 70 °C. After the dyeing the fabrics were washed for 30 minutes, by 70–80 °C and dried.

The Bruker (Vektor 22) FTIR spectrometer with the ATR attachment with a ZnSe crystal was used for the FTIR analysis of cotton fabrics.

The values of dry and wet rubbing fastness of cotton fabrics were measured by using the Stainingtester FD 17 equipment. The measuring was doing according to the Standard STN EN 20105-A03 and STN EN ISO 105-X12.
The cotton samples were submitted to abrasion by dry and wet cotton woven fabrics. Degree of bleeding colour from dyed cotton fabrics to the white cotton fabrics were specified by using grey scale.

Results and discussion

The results of % of exhaustion dyeing of plasma treated and untreated cotton fabrics are shown in Fig. 1.

At the dyeing temperature 60 °C and dyeing time 30 minutes the percentage of exhaustion dyeing are lower for plasma treated samples. On the other hand at higher dyeing time the percentage of exhaustion dyeing is decreasing for 10 and 20 minutes ageing time in comparison to untreated sample. But at the dyeing of cotton fabrics after 30 mins since plasma treatment the percentage of exhaustion dyeing is better than untreated fabric.

At the dyeing temperature 70 °C and dyeing times 30 minutes and 60 minutes there can observe the improving of dyeing cotton fabrics by using plasma treatment. The deyability is better for dyeing time 60 mins and ageing time 30 mins.

From results of dyeing cotton fabrics is obvious that increasing dyeing temperature decrease the dyeability of

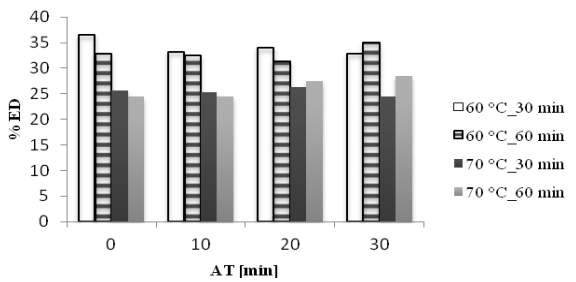

Fig. 1. **Exhaustion dyeing of untreated and plasma treated cotton fabrics after various ageing time**

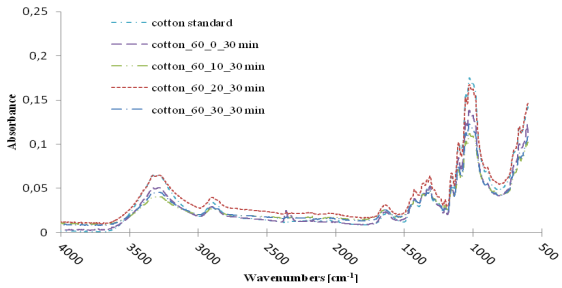

Fig. 2. **FTIR spectrum of untreated and treated cotton fabric, dyeing for 30 min by 60 °C**

Table I
The dry and wet rubbing fastness of cotton fabrics. Dyeing time 30 min and dyeing temperature 60 °C

AT [min]	Rubbing fastness			
	Dry		Wet	
	Before cleaning	After cleaning	Before cleaning	After cleaning
0	4-5	5	1-2	3-4
10	5	5	2-3	3-4
20	5	5	2	3-4
30	5	5	3-4	3

Table II
The dry and wet rubbing fastness of cotton fabrics. Dyeing time 60 min and dyeing temperature 60 °C

AT [min]	Rubbing fastness			
	Dry		Wet	
	Before cleaning	Before cleaning	Before cleaning	Before cleaning
0	5	5	2	3
10	5	5	3	3
20	5	5	2-3	3
30	5	5	2-3	3-4

Table III
The dry and wet rubbing fastness of cotton fabrics. Dyeing time 30 min and dyeing temperature 70 °C

AT [min]	Rubbing fastness			
	Dry		Wet	
	Before cleaning	Before cleaning	Before cleaning	Before cleaning
0	5	5	3	4-5
10	5	5	3	5
20	5	5	3-4	5
30	5	5	3	5

Table IV
The dry and wet rubbing fastness of cotton fabrics. Dyeing time 60 min and dyeing temperature 70 °C

AT [min]	Rubbing fastness			
	Dry		Wet	
	Before cleaning	Before cleaning	Before cleaning	Before cleaning
0	5	5	3	4
10	5	5	3-4	3-4
20	5	5	3-4	4-5
30	5	5	3-4	4-5

untreated as well as plasma treated samples.

Plasma treating is the most efficient at 30 mins of ageing time for dyeing temperatures 60 and 70 °C.

FTIR spectrum shows that plasma treatment did not lead to greater changes in functional groups between untreated cotton fabrics before dyeing and treated cotton fabrics after dyeing.

The dry and wet rubbing fastness of cotton fabrics before and after cleaning which were dyed after various ageing time are in the Tables I–IV.

The obtained results have shown that the dry rubbing fastness for all samples before and after cleaning is 5 which means that colour was not bleeding from dyed cotton fabrics to the white cotton fabric.

The wet rubbing fastness before and after cleaning is lower compare to dry rubbing fastness. It means that unbounded dye molecules diffused from cotton to cleaning bath.

The rubbing fastness improves for treated fabrics after cleaning and it improves with increasing ageing time.

Results confirm that rubbing fastness of cotton fabrics which were dyed 30 and 60 minutes at 70 °C temperature is higher than at 60 °C. The cleaning improves the quality of dyeability of cotton fabrics what is confirmed by higher rubbing fastness at longer dyeing time.

Conclusions

The plasma treatment has positively effect to dyeability of cotton fabrics for both dyeing temperatures and at the higher dyeing time.

Dry rubbing fastnesses do not depend on the type of plasma ageing time before and after cleaning.

The plasma surface modification and higher dyeing temperatures improve the wet rubbing fastness.

ITMS 262202220134 VY-INTECH-TEX.

REFERENCES

1. Walk R. M., et al: Journal of Pediatric Surgery *48*, 67 (2013).
2. Kizling M. B., et al: Appl. Catal. A: General *147*, 1 (1996).
3. Karahan H. A., et al: Coloration Technol. *124*, 106 (2008).
4. Wang C. X., et al: Surf. Coat. Technol. *201*, 6273 (2007).

P-50

DETERMINATION OF POLYOLEFINS' ODOUR PROPERTIES IN CONNECTION WITH C-EMISSIONS

ANITA VÍGHOVÁ, EVA LUKÁČOVÁ*, ZUZANA WETTEROVÁ, and RÓBERT POLNIŠER

SLOVNAFT, a.s., Quality Control Petchem, Vlčie Hrdlo 1, 824 12 Bratislava, Slovakia
anita. vighova@slovnaft.sk

One of the most important characteristics in vehicle interior is polymer´s parts smell. It is the main criterion during the selection of polymers suitable for using in automotive industry, as far as the polymers comprise more than 50 % of cars' construction. Subject is focused on the sensory testing by human and determining the C-emissions by GC-Headspace[1].

Volatiles may contain residual monomers, additives, moisture, solvents, residual catalysts, decomposition products of resins and their additives and can be associated with odour and off-taste in packaging foodstuffs[2].

Determination of polyolefin's odor properties is based on assessing the sensory characteristics of pellets/ films/ other forms of plastic materials or additives by mean of the increased or in special case room temperature, from which the released volatile substances may show detectable odour. Samples are tested in the 1 litre test bottle (glass and perfectly odour neutral). The intensity of odour is marked by at least 3 trained and verified workers according to established "intensity scale from 1 to 6" (ref.[3]). For polyolefin used in automotive industry is the maximum allowed intensity scale mark for pellets 3 and for films or the other forms 3.5.

The identifications of emitted substances generated during polymer production or processing is critical for material safety, health and environmental aspects. A wide range of polyolefin was studied, because the automobile indoor air quality influences comfort, interior microenvironment, safety and health. Whilst by the sensory testing we can detect just smelly odours the others (from time to time much more interesting) are hardly detected and therefore the analytical method – determining of C-emissions was developed.

C – emissions are evaluated from final pellets by method designed for GC/Static Headspace with Flame Ionization Detector (FID). Exact amount of sample is preheated in glass vials for specific time and temperature. Organic compounds are evaporated from the heated sample and released into the space above pellets. When equilibrium is reached, the concentration of the volatiles in the headspace is at its maximum and it is injected onto the analytical column for separation Then the C – emissions potential is measured on the basis of the sum of all values provided by the emitted substances after gas chromatography analysis and flame ionization detection.

Still we can say that polymers vary their composition like their chemical structure and could emit chemical

substances, compounds into the air inside the car. The concentration of emitted volatile compounds is influenced by the individual sources in the interior equipment, outdoor and indoor air contaminants, and interior sources, internal parts exposed to the heat and ventilation conditions. Significant concentration of volatile organic compounds can be present in the interior of vehicles due to emissions from materials which are part of the interior fittings[2].

REFERENCES

1. VDA 277, *Determination of emission of organic compounds*, 1995.
2. C. Henneuse-Boxus, T. Pacary: *Rapra Review Reports*, Volume 14, Number 5, 2003.
3. VDA 270, *Determination of the odour characteristics of trim materials in motor vehicles*, 1992.

P-51

MODIFICATION OF BIODEGRADABLE CHITOSAN SCAFFOLD

MIROSLAVA VITTEKOVÁ, MÁRIA HNÁTOVÁ, KATARÍNA KOMAROVÁ, and DUŠAN BAKOŠ

Institute of Polymer Materials, Faculty of Chemical and Food Technology, Slovak University of Technology, Radlinského 9, 812 37 Bratislava, Slovak Republic
miroslava.vittekova@stuba.sk

Introduction

Chitosan is interesting biopolymer predestined for biomedical applications due to its properties (easy to fabricate, film and fiber-forming, excellent biological properties – biocompatibility, bioresorption, antimicrobial properties). Cationic character of chitosan is used for complex formation with anionic polymers, as well as amino-groups on chain can be used for chemical modification and crosslinking, e.g with dialdehydes, through the formation of Schiff base[1].

Cyclodextrins have been studied intensively as carriers of bioactive substances. Cyclodextrins are natural, from starch derived oligosaccharides. They are composed of α-1,4-linked D-glucose units with arrangements containing a hydrophobic internal cavity that can act as a host for various, generally lipophilic, guest molecules[2]. Salicylic acid has favorable pharmacological effects and also is able to create a cyclodextrin inclusion complex[3].

The work is focused on the study of biodegradable chitosan scaffold modified by molecules of *β*-cyclodextrin and cross-linked with poly-dialdehyde of starch. One of the aims of this work has been to study the influence of added components on surface energy and properties of scaffolds. UV/VIS spectrophotometry was used in order to determine quantitatively sorption of salicylic acid on the lyophilized matrixes or on nonwoven layers from nano-fibres of poly (vinyl) alcohol (PVA) and poly(glycolic-lactic) acid (PLGA) prepared by electrospinning and coated with the film of *β*-cyclodextrin and chitosan.

Materials and methods

High molecular chitosan (Shanghai Hong Yea Food Co., Ltd.), *β*-cyclodextrin (*β*-CD) (Sigma-Aldrich Co., USA) and starch poly-dialdehyde (DS) (FCHPT STU BA) were used. Salicylic acid (SA) was supplied by Mikrochem s.r.o., Pezinok, Slovakia. Non-woven fabric – polymeric carrier consisted of two parts – the non-woven liner (PP), on which two types of polymer nanofibers were applied (PVA and PLGA), made in SPUR a.s. Zlín, Czech Republic.

Chitosan scaffolds and films preparation

Chitosan solution (2 wt.%) was prepared by dissolving of polymer in 0.5 M acetic acid at the laboratory temperature. *β*-CD solution in deionized water at the concentrations 6, 9 and 18 g l^{-1} was added to chitosan solution and mixed together. 1.3 wt.% DS solution was used as crosslinking agent of scaffolds and films at the content gradually increased from 1 to 4 wt. % in regard to the total amount of polymer and CD. Films from such mixture were dried at 37 °C and scaffolds were prepared after freezing the mixture by lyophilizing in JOUAN LP3 equipment at –47 °C for 19–24 hours. The surface of nano-fibres layers was covered by film soaking them in 0.5 wt.% solution of chitosan with *β*-CD of concentration 18 g l^{-1} and drying at 37 °C.

Measurement of surface energy

Surface energy was measured on chitosan-CD films on both sides using the drops method. The samples were prepared by chitosan film cutting into thin strips. Drops with volume of 5 μl were applied on samples. Each measurement was repeated five times. Photos of all samples were taken with a CCD camera with SEE System. Surface energy of the solid test samples was calculated according to the Owens-Wendt method.

Swelling

The measurements were performed on lyophilized scaffolds. Deionized water was used as swelling medium. Samples were swelled in medium at room temperature for 30 seconds. Comparing to dry sample, the water content was recalculated to 1 g of sample.

UV/VIS spectrophotometry

Absorption spectra of all samples were recorded by UV/VIS spectrophotometer CECIL CE 7450 in the wavelength range 220–360 nm in *n*-hexane.

SA sorption measurements

Two solutions of SA (1.0 mM and 0.5 mM) were used for sorption measurements. Scaffolds with crosslinked agent (1 wt.%) and different *β*-CD concentrations (6, 9 and 18 g l^{-1}) were evaluated after their dipping during 24 hours at the room temperature.

Nanofiber layers were soaked in the solution of 0.5 mM SA for 5 hours. Decrease of solution concentration after

sorption was monitored after 1, 2, 3, 4 and 5 hours using UV/VIS spectrophotometry.

Results and discussion

16 lyophilized chitosan scaffolds and chitosan model films modified with *β*-CD and crosslinked with DS were examined to evaluate DS and CD concentrations influence on surface energy.

From measurements of the surface energy of solid films at different concentrations of both DS and CD, it can be seen in Fig. 1 that increasing concentration of *β*-CD at all concentrations of crosslinking agent DS increase surface energy measured on front sides. From this, probably *β*-CD presence on the film surface can change a surface structure and with increasing amount of *β*-CD molecules the surface is more hydrophilic.

Results obtained from swelling measurements of lyophilized scaffolds showed that to be able to express an influence of *β*-cyclodextrin on swelling, scaffolds should be sufficiently crosslinked (higher amounts of DS) as can be seen from Fig. 2. It was confirmed that higher concentration of *β*-CD in the scaffold composition, the higher amount of water accepts.

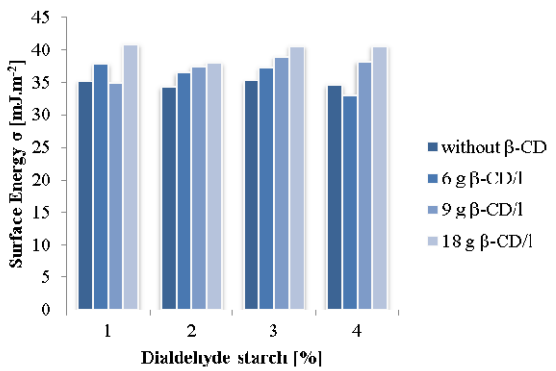

Fig. 1. **The dependence of surface energy of films measured on the front side at different concentrations of DS and *β*-CD**

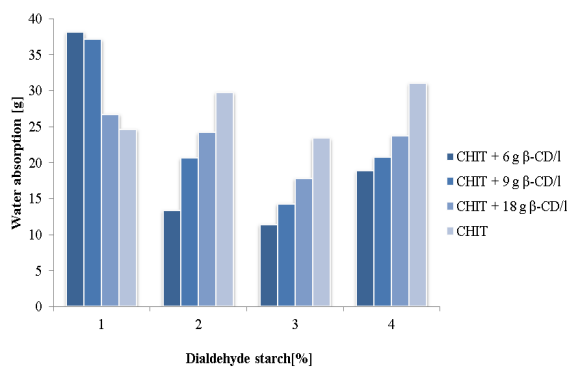

Fig. 2. **The dependency of accepted water on scaffold composition**

Fig. 3. **The comparison of the sample volume before and after swelling**

During swelling chitosan scaffold samples the volume increased very quickly and swelled samples were twice larger (Fig. 3).

The sorption experiments of chitosan scaffolds of different composition from SA solutions showed that the concentration of SA in the solution after long time (at least 24 hours) decreased. The results of sorption measurements were obtained comparing values on constructed calibration curve of reference solutions (Fig. 4).

Increased soaking time led to absorbance decreasing with a reduction of SA concentration in solution. Probably, there is an inclusion of SA into the *β*-CD hydrophobic cavity on the scaffold surface. On the other hand, adsorption on the chitosan molecule is not avoided.

The results of sorption measurements on nano-fibres layer showed an importance of chitosan film deposition with *β*-CD on the nano-fibres (sorption on this film). It can be assumed that the sorption, as is documented in Fig. 5 and 6, is connected with inclusion of SA molecules into the *β*-CD cavity. These results were compared to unmodified nano-fibres layers where sorption of SA did not observed.

Conclusion

The results show that scaffolds must be sufficiently crosslinked and the active substances which contents must be well dispersed to reach a positive influence on required scaffolds properties. The concentration range of solutions

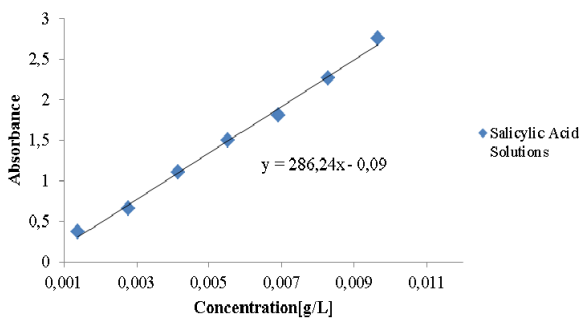

Fig. 4. **The calibration curve of SA solutions**

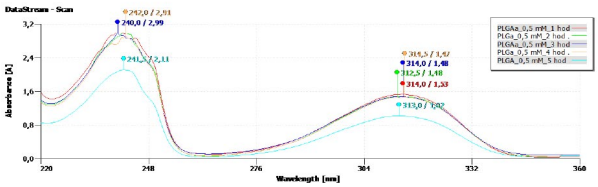

Fig. 5. **The changes in UV spectrum after SA sorption from 0.5 mM solution on PLGA layer**

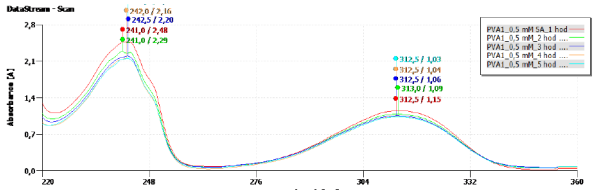

Fig. 6. **The changes in UV spectrum after SA sorption from 0.5 mM solution on PVA layer**

used was sufficient for sorption of the active substance SA on scaffolds or nano-fibres layers connected with inclusion to *β*-CD cavity. Environment of *n*-hexane as a solvent in this case was the model as experiments were focused on characterization of materials in solid form. Results showed the importance of modifications of chitosan with CDs and further study to clarify sorption of other bioactive substances in such systems will be valuable.

REFERENCES

1. Rinaudo M.: Progress Polym. Sci. *31*, 603 (2006).
2. Manakker F., Vermonden T., Nostrum C. F., Hennink W. E.: Biomacromolecules *10*, 3157 (2009).
3. Mahdí J. G.: J. Saudi Chem. Soc. 14 (2010).

P-52

MODIFICATION OF ACRYLONITRILE-BUTADIENE RUBBER COMPOUND BY NANOCLAY AND SILICA

ZDENĚK ZÁVORKA[a] and JIŘÍ MALÁČ [b]

[a] Department of Polymer Engineering, Faculty of Technology, Tomas Bata University in Zlin, 762 72 Zlin, [b] Centre of Polymer Systems, University Institute, Tomas Bata University in Zlin, Nad Ovcirnou 3685, 760 01 Zlin, Czech Republic
z.zavorka@seznam.cz

Introduction

The cooling effect of air conditioning (A/C) systems is typically achieved by a hydro-fluorocarbon refrigerant such as 1,1,1,2-Tetrafluoroethane (R-134a). However, R-134a has a very high relative global warming potential (GWP) and will be restricted after 2016 (ref.[1]). One of the proposed replacements is 2,3,3,3-Tetrafluoropropene (HFO-1234yf) developed by E.I. duPont deNemours and Honeywell International.

Due to differences in molecular composition and size permeation through rubber sealing components increases by about 30% when compared to the current R-134a (ref.[2]). This demonstrates the challenges and importance of improving permeation behavior of rubber compounds for future use with low GWP refrigerants without sacrificing mechanical properties necessary for sealing performance.

Improving permeation resistance of these rubber materials can be achieved by proper selection of the "white fillers" added to the rubber compound. Specially, permeation resistance can be improved by utilizing common fillers with plate-like structure such as kaolin, clay and talc. While these fillers tend to be cost effective, they may cause unacceptable deterioration of the mechanical properties of the rubber compound[3]. Addition of nanoclay fillers appears to offer both reduced permeation rates for refrigerant and improvement of mechanical properties.

Combination of silica and nanoclay was subject of our study and our effort to identify the most cost effective A/C rubber compounds which optimize both mechanical properties and permeation resistance. Combinations of silica, kaolin and talc were investigated in parallel as low cost solutions and compared with silica and nanoclay combinations in their effect on property modification.

Experimental

Mineral materials used:

- Nanoclays Cloisite® 15A, 20A, 25A, 93A, Na+
- Nanofil® 5 (Sud-Chemie)
- Kaolin – type KKAKA (LB Minerals Kaznejov)
- Calcinated kaolin PO5 + (Ceske lupkove zavody)
- Talc – type 1.A (Demerska Hnusta)

Formulations of rubber compounds are shown in Table I.

Table I
NBR compound formulations

Chemical	No. 1 [phr]	No. 2 to 10 [phr]
NBR Krynac® 33.45	100	100
Silica Perkasil® KS 300	30	30
Oil	20	20
Nanoclay, kaolin or talc	–	10
Norperox BIBP 40	7	7
Rhenofit TAC/GR 70	2	2
Total	159	169

Measurements

Vulcanization characteristics were determined by a RPA 2000 at temperature 175 °C. Dynamic-mechanical properties were consequently tested at temperatures 40, 70 and 120 °C in constant strain amplitude of 1 % with constant oscillation frequency 0.3 Hz

Tensile strength and elongation were determined according to ISO 37 on an Alpha Technologies Tensometer 2000 test machine at 23 °C. Hardness durometer (Shore "A scale) was measured according to standard ISO 7619-1.

Permeation of refrigerant R-134a through samples of vulcanized rubber was measured utilizing a photoacoustic spectrometer (Innova model 1314) at a pressure 2 MPa and temperature 70 °C. The test was done according to European Union Commission Regulation (EC) No 706/2007 (ref.[4]).

Results and discussion

As it is shown in Fig. 1 and 2, the addition of all types of tested nanoclay fillers resulted in significant increase in hardness, tensile strength and elongation except nanoclay Cloisite Na+.

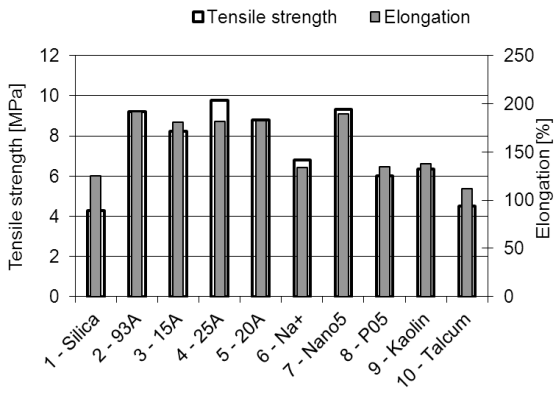

Fig. 1. **Comparison of tensile strength and elongation**

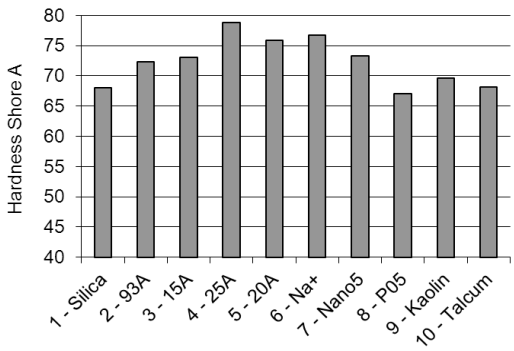

Fig. 2. **Comparison of hardness**

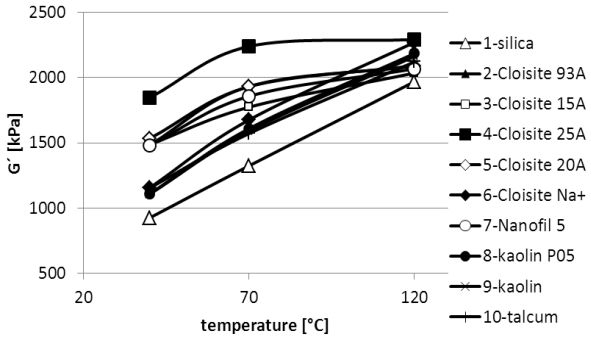

Fig. 3. **Dependence of dynamic storage shear modulus G' on temperature**

The improvement could be caused by the higher aspect ratio of exfoliated nanoclays compared to silica or common white fillers.

The results in Fig. 3 reveal that dynamic storage modulus in shear (G') for compounds with nanoclays increases to temperature of approximately 70 °C, where G' begins to level off. It is possible that NBR chains are intercalated into the structure of the nanoclay filler and as the temperature increases above 70 °C, the chains are released. This figure shows a linear increase of dynamic modulus G´ with temperature for compounds with silica, kaolin and talc, due to the different particle structure of the fillers.

Fig. 4 reveals that the addition of nanoclay significantly improves gas barrier properties, which manifests itself through a reduction in permeation. As can be seen, the permeation of refrigerant R-134a decreased by 15–30 % after addition of nanoclays into compound of NBR and silica. The reduction is probably caused by plate-like shape of exfoliated nanoclays created more tortuous pathways which the refrigerant molecules must travel to diffuse through the

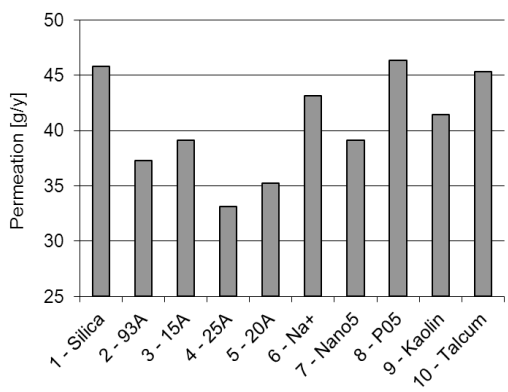

Fig. 4. **Comparison of refrigerant R-134a permeation**

material. Exfoliated nanoclays should also reduce the diffusion coefficient by restriction of motion of NBR chains[5]. The recent research has shown that the higher aspect ratio fillers are the key factor to reduce gas permeation through nanocomposites[6,7] and the results presented in this paper agree with this conclusion.

Conclusion

The objective of this study was to reduce permeation of refrigerant R-134a through NBR rubber by using suitable combination of fillers in NBR compounds, without significantly degrading mechanical properties. Nanoclay fillers demonstrated the ability to provide a 30 % reduction in permeation and achieving improved mechanical properties. The key to obtaining these enhancements was adequate level of exfoliation and polymer-filler interaction of the nanoclay fillers, confirmed by dynamic-mechanical measurements.

This exfoliation and interaction was dependent on the type and amount of the nanofiller modifier. Cloisite Na+ is the unmodified nanoclay and in the NBR compound gives properties similar to common white fillers as talc and kaolin. On the other hand, Cloisite 20A and 25A contain the same modifier at different levels. The good performance of the Closite 25A with a higher modifier level led to the best results seen in this study. Combinations of nanoclay with silica enhanced exfoliation during mixing of the compounds due to the increase of viscosity caused by presence of silica.

Application of nanoclay Cloiste 25A with silica has shown to be a combination that results in a compound with higher permeation resistance to R-134a and improvement in tensile strength, elongation and dynamic modulus of rubber compound for sealing applications in the automotive A/C systems.

REFERENCES

1. Directive 2006/40/ec of the european parliament and of the council relating to emissions from air-conditioning systems in motor vehicles and amending Council Directive 70/156/EEC, 17 May 2006
2. Sae cooperative research program 1234-2: Material compatibility of HFO-R1234yf (final report), 2008
3. Ducháček V.: *Světlá plniva*, Česká společnost průmyslové chemie, Praha 2010.
4. Commission regulation (EC) No 706/2007 – laying down, pursuant to Directive 2006/40/EC of the European Parliament and of the Council, administrative provisions for the EC type-approval of vehicles, and a harmonised test for measuring leakages from certain air conditioning systems, 21 June 2007
5. Yurong Liang, Yiqing Wang, Youping Wu, Yonglai Lu, Huifeng Zhang, Liqun Zhang: Polymer Testing *24*, 12 (2005).
6. K. Ynao, A. Usuki, A. Okada, T. Kurauchi, O. Kamigatio: J. Polymer Sci.: Part A: Polymer Chemistry *35*, 2289 (1997).
7. T. Lan, P. D. Kavirtana, T. J. Pinnavaia: Chem. Mater. *6*, 573 (1994).